

FAST TRACK COMMUNICATION

RE L₃ x-ray absorption study of REO_{1-x}F_xFeAs (RE = La, Pr, Nd, Sm) oxypnictides

B Joseph¹, A Iadecola¹, M Fratini², A Bianconi¹, A Marcelli³ and N L Saini¹

¹ Dipartimento di Fisica, Università di Roma 'La Sapienza', Piazza le Aldo Moro 2, 00185 Roma, Italy

² Istituto di Fotonica e Nanotecnologie, CNR Roma, Italy

³ Laboratori Nazionali di Frascati, INFN, 00044 Frascati, Italy

Received 4 August 2009, in final form 22 September 2009

Published 8 October 2009

Online at stacks.iop.org/JPhysCM/21/432201

Abstract

Rare earth L₃-edge x-ray absorption near-edge structure (XANES) spectroscopy has been used to study REOFeAs (RE = La, Pr, Nd, Sm) oxypnictides. The Nd L₃ XANES due to the 2p_{3/2} → 5εd transition shows a substantial change in both white line (WL) spectral weight and the higher energy multiple scattering resonances with the partial substitution of O by F. A systematic change in the XANES features is seen due to varying lattice parameters with ionic radius of the rare earth. On the other hand, we hardly see any change across the structural phase transition. The results provide timely information on the local atomic correlations showing the importance of the local structural chemistry of the REO spacer layer and interlayer coupling in the competing superconductivity and itinerant striped magnetic phase of the oxypnictides.

1. Introduction

Recently, the discovery of high temperature superconductivity in the Fe-based oxypnictides [1] has attracted wide attention from the condensed-matter community. The rare earth (RE) oxypnictides (REOFeAs) have a layered structure, similar to the copper oxide superconductors and diborides, with electronically active (FeAs)^{δ-} layers separated by (REO)^{δ+} reservoirs. Both the charge transfer and the lattice misfit between the two sub-layers [2, 3] are important for the superconducting function of these materials, similar to the case of cuprates [4, 5] and diborides [6]. The REOFeAs become superconducting with a maximum transition temperature $T_c \approx 55$ K [7, 8] when the active layers are doped through atomic substitutions or oxygen vacancies in the REO spacers. One of the interesting aspects of these materials is the competing spin density wave (SDW) and superconductivity [8–11]. Indeed, the undoped compound REOFeAs is antiferromagnetically ordered (albeit a poor metal), however at the same time showing a structural phase transition from the tetragonal to the orthorhombic phase [12, 3, 13]. With doping the system

becomes superconducting and the structural transition as well as the SDW transition disappear [8, 14–16]. In addition, while the maximum T_c of the doped system increases with reducing RE ion size [7, 17], the structural transition temperature (T_s) decreases for the undoped system [3]. This further underlines the importance of the local chemistry of the REO layers in the correlating itinerant magnetism and superconducting function of these materials.

It is well known that RE L₃ x-ray absorption near-edge structure (L₃-XANES) spectroscopy is a direct probe of the local structure around a selected absorbing atom and of the distribution of the valence electrons, with the final states in the continuum being due to multiple scattering resonances of the photoelectron in a finite cluster [18]. Moreover, in an ordered structure, the focusing effects of atoms in a collinear geometry also determines multiple scattering resonances in a large cluster of near neighbor atoms. Therefore the RE L₃-XANES is an ideal tool to study the local geometry around the RE and has often been applied to study rare earth containing materials [19–21]. The added advantage of this technique lies in the fact that, unlike photoemission experiments, there are

negligible surface effects (and multiplet effects), making it a very useful finger print probe of unoccupied valence states and the local chemistry of the absorbing atom.

Here we have exploited RE L_3 -XANES spectroscopy to make a systematic study of the local geometry around the RE atom and the related electronic structure, measuring a series of REOFeAs (RE = La, Pr, Nd and Sm) with varying rare earth size. We have also studied the effect of the tetragonal to orthorhombic structural phase transition as well as the superconductivity on the RE L_3 XANES. We find a systematic change in the L_3 -XANES spectra reflecting the varying electronic and local geometrical structure of the title system. Incidentally the L_3 -XANES white lines hardly show any change across the tetragonal to orthorhombic structural phase transition temperature, however, a clear change is observed with the electron insertion by F-substitution. The results suggest that, in addition to the FeAs layers, structural coupling with the spacer layer should be important for the high T_c , reminiscent of the recent debate on misfit strain [5, 4, 6] and out-of-plane disorder [22–24] controlling superconductivity in the copper oxide perovskites.

2. Experimental details

RE L_3 -edge x-ray absorption near-edge structure (L_3 -XANES) measurements were performed on powder samples of REOFeAs (RE = La, Pr, Nd, Sm) prepared using a solid state reaction method [25]. Prior to the absorption measurements, the samples were characterized by x-ray diffraction for their structural properties [3]. The structural phase transition temperatures were measured to be 165 K, 155 K, 135 K and 130 K respectively for the La, Pr, Nd and Sm containing REOFeAs samples. The superconducting transition temperature for the F-doped $\text{NdO}_{1-x}\text{F}_x\text{FeAs}$ was found to be 49 K [26]. The x-ray absorption measurements were made at the XAFS beamline of the Elettra Synchrotron Radiation Facility, Trieste, where the synchrotron radiation emitted by a bending magnet source was monochromatized using a double crystal Si(111) monochromator. The L_3 -XANES measurements were made at two temperatures (room temperature and 80 K) in the transmission mode using three ionization chambers mounted in series for simultaneous measurements on the sample and a reference. For the low temperature measurements, the samples were mounted on a liquid nitrogen cryostat cold finger enclosed in an Al shroud with a Be window. The sample temperature was measured to be 80 ± 1 K for the low temperature measurements. As a routine experimental approach, several absorption scans were collected to ensure the reproducibility of the spectra, in addition to the high signal to noise ratio.

3. Results and discussion

Figure 1 shows normalized RE- L_3 spectra of REOFeAs (La, Pr, Nd, Sm) measured at room temperature showing an intense peak, the characteristic white line (WL) of RE^{3+} . Here, the zero of the energy scale is fixed to the WL peak position for a proper comparison between the different spectra. It is worth

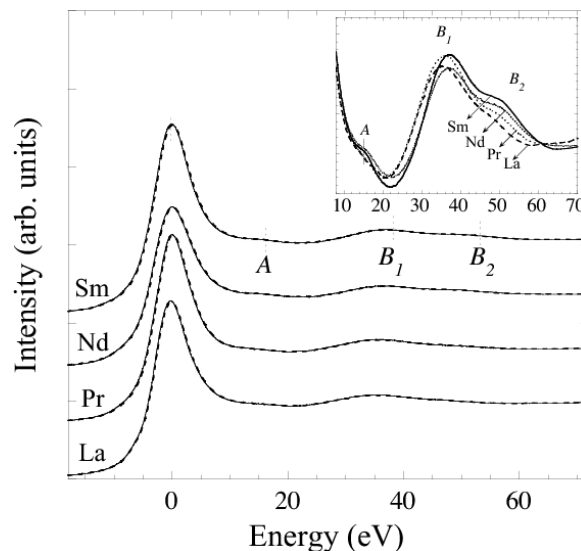


Figure 1. The near-edge regions of the normalized RE L_3 -edge absorption spectra of the REOFeAs at 80 K and room temperature (solid and dotted lines, respectively). The zero of the energy scale is fixed to the characteristic WL representing $2p_{3/2} \rightarrow 5d$ transitions. Other near-edge features are assigned as A, B_1 and B_2 , showing a change of local geometry with changing rare earth. The inset shows a zoom over the near-edge features A, B_1 and B_2 (room temperature).

recalling that the L_3 absorption process is a $2p_{3/2} \rightarrow 5\epsilon d$ (or $2p_{3/2} \rightarrow 6\epsilon s$) transition governed by the dipole selection rules ($l = \pm 1$) and hence empty states with d or s symmetries (and admixed states) can be reached in the final state. Since the probability for a $2p_{3/2} \rightarrow 6\epsilon s$ transition is about two orders of magnitude lower than for a $2p_{3/2} \rightarrow 5\epsilon d$ transition, the earlier can be ignored for describing the L_3 WL. The one-electron picture (i.e., all the orbitals not directly involved in the absorption process are passive in the final state) works well for the L_3 WL unless the materials of interest are mixed valent systems. In the present case, the WL appears to be a typical of RE^{3+} and hence the one-electron picture could be fairly used to describe the spectra.

In addition to the intense WL, we can see different near-edge features, a weak structure around 15 eV above the WL (feature A), and the continuum resonances appearing as a two peak structure (the broad features denoted by B_1 and B_2 appearing respectively around 35 and around 50 eV) due to the photoelectron scattering with the nearest neighbors. The RE atoms have 4 near neighbors O sitting at a distance ≈ 2.3 Å and 4 As atoms occupying a site at ≈ 3.3 Å, and hence the two peak structure of the continuum resonance is expected with the low and high energy peaks due to As and O scattering respectively. The energy separation between the two is consistent with the $\Delta E \propto 1/d^2$ relation for a continuum resonance [27]. Here it is worth referring to Ignatov *et al* [28] reporting the La L_3 -XANES on LaOFeAs with a typical La^{3+} WL and the continuum peak, however, with a limited discussion they have incorrectly assigned the continuum resonance peak B_1 to the La–O distance.

The feature A is very weak or absent for the La and Pr L_3 -XANES while clearly visible for the Nd and Sm L_3 cases (see

e.g., the inset). The feature A has been frequently observed in the L_3 -XANES of the rare earths and discussed as being due to a particular local structural geometry of the RE [29]. Here the feature A is found to be absent (or very weak) in the La and Pr L_3 spectra while clearly seen in the Nd and Sm L_3 edges. The feature A is found to appear at the same energy. Indeed, the observation is consistent with the earlier results [29, 30], albeit with a dubious interpretation relating it to the local structure. Considering the fact that the basic geometry of the RE is the same, it is difficult to rule out feature A as having an electronic origin or being related to disorder in the REO layer, however, detailed multiple scattering calculations should be performed for further clarification.

On the other hand, the continuum resonance peaks B_1 and B_2 show a systematic change with the rare earth ion size (see e.g. the inset) indicating a clear evolution of the local geometry around the RE. Peaks B_1 and B_2 shift towards higher energy due to decreasing RE–As and RE–O distances with decreased rare earth size, consistent with the $\Delta E \propto 1/d^2$ empirical rule [27]. It is interesting to note that neither the WL nor the XANES features show any appreciable change across the tetragonal to orthorhombic structural transition temperature (dotted and solid lines in figure 1). Therefore, while the average symmetry measured by diffraction (long range ordered structure) changes, the local atomic structure measured by the XANES hardly show any change except a thermal shrinkage of the lattice (figure 2). On the other hand, the negligible change in the WL intensity suggests that the electronic structure of the unoccupied RE d-states (and admixed electronic states) remains the same in the two structural phases. This observation is consistent with the Fe K-edge XANES [31] study revealing hardly any change in the local structure across the structural phase transition in these materials. However, the Fe K-edge study has revealed a clear change in the $1s \rightarrow 3d$ quadrupole transition (albeit small) across the structural phase transition. Thus, it is possible that the tetragonal-to-orthorhombic structure phase transition is being induced by the electronic part, due to the fact that the electronic states near the Fermi surface are mainly of Fe 3d nature. However, more work is necessary to discuss the structural phase transition versus local structure by XANES, enhanced by polarized data.

Figure 2 shows energy positions of the peak B_1 with respect to the WL (ΔE) at two temperatures, showing a continuous increase with decreasing rare earth size due to the decreased RE–As distance. The ΔE at low temperature is slightly higher by almost the same amount, suggesting an average but similar unit cell shrinkage for all the samples on lowering the temperature. We have also plotted the crystallographic RE–As distance at room temperature for comparison (lower panel). The inset displays the ΔE as a function $1/d^2$, showing the expected linear behavior [27].

To get further information from the L_3 -XANES, we have extracted the line shape parameters for the WL as well as the peaks B_1 and B_2 . In the one-electron approximation the L_3 -XANES WL could be deconvoluted by a Lorentzian (core hole life time), convoluted by the experimental broadening providing the 5d (and admixed) density of empty states

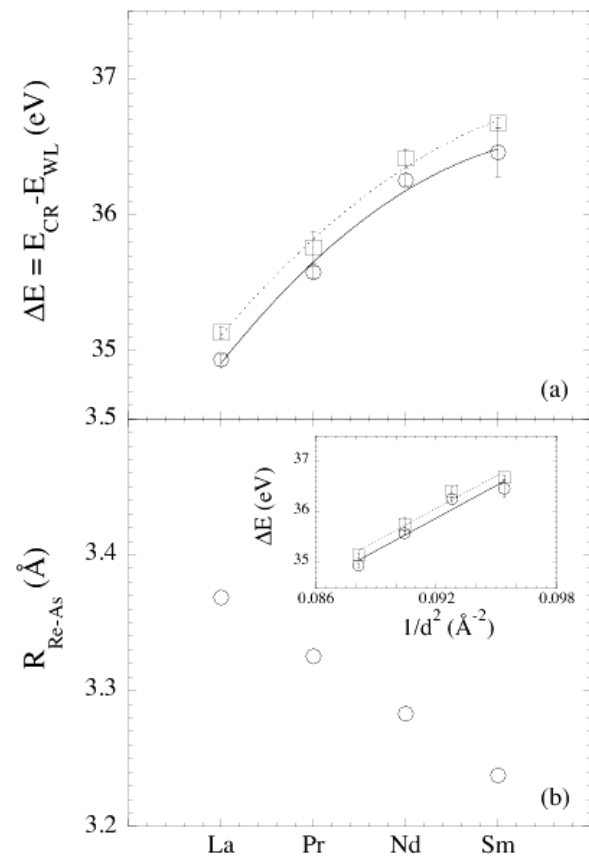


Figure 2. Energy separation between the white line and the continuum resonance peak B_1 (ΔE) at room temperature (open circles) and at 80 K (open squares), showing a continuous increase with decreasing rare earth size due to decreased RE–As distance (a). The energy positions are determined from the second derivative of the L_3 XANES. The crystallographic RE–As distance at room temperature is also shown for comparison (b). As expected, a linear relation is observed between the ΔE and $1/d^2$ (see the inset in (b)). The error bars represent the standard deviation estimated using different experimental scans.

weighted by the matrix element and the arctan curve to take into account the transition into the continuum. The energy positions are similar to those which have been obtained from the second derivative of the spectra (figure 2). All efforts were made to take care of experimental aspects influencing the L_3 -line shapes (thickness and homogeneity of the samples), however, it is not correct to consider equal transition matrix elements for all the rare earths, therefore the absolute intensities can not be compared quantitatively as a function of the RE. Moreover, the absolute intensity of the WL does not show any appreciable or systematic change with the rare earth. On the other hand, the intensities of the continuum resonance peaks B_1 and B_2 , probing the local geometry around the rare earth atom, change systematically. The relative change in the intensity of peaks B_1 and B_2 , defined as $\Delta I = [I(B_1) - I(B_2)]/[I(B_1) + I(B_2)]$, is displayed in figure 3 as a function of rare earth, showing a decrease with decreasing rare earth size, revealing a systematic change of local geometry around the RE involving the As and O atoms (peak B_1 is due to the RE–As distance while peak B_2 is due

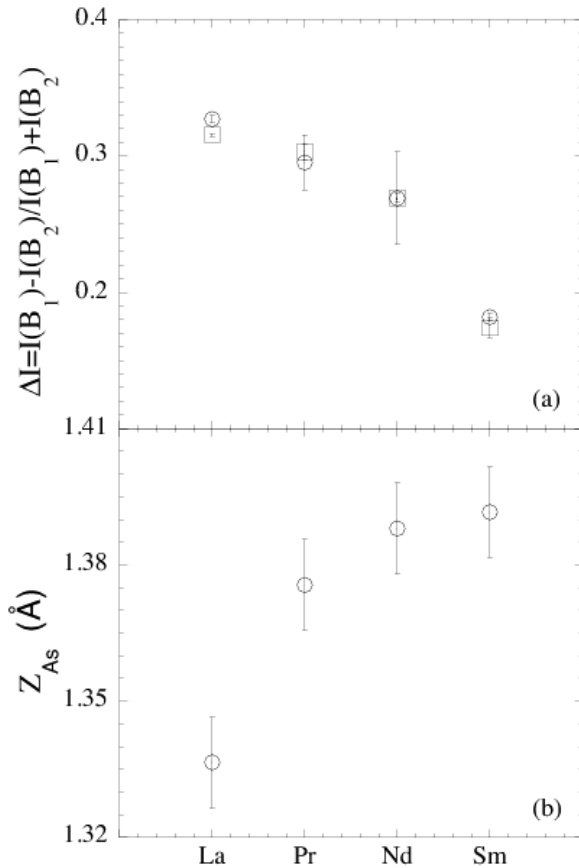


Figure 3. Difference of relative intensities of the continuum resonances B_1 and B_2 as a function of rare earth (a). The vertical position of the As atom with respect to the Fe–Fe plane, measured by the Fe K-edge EXAFS [32], is also shown (b).

to the RE–O distance). Since the RE–As represents out-of-plane atomic correlation while the RE–O describes in-plane correlation, the decreasing ΔI should reflect the increased correlation between the RE–O layer and the Fe–As layer (i.e., increased interlayer coupling) with decreasing rare earth size. Although it is difficult to quantify the atomic displacement pattern around the RE, the results seem to be consistent with the higher perpendicular position of the As atom with respect to the Fe–Fe plane (figure 3(b)) and the decreased RE–As distance (figure 2(b)) with decreasing rare earth size.

Let us turn to the effect of doping on the L_3 -XANES. To explore this, we have used NdOFeAs as a representative and measured Nd L_3 -XANES on the undoped and F-substituted system. Figure 4 shows the measured Nd L_3 -XANES at room temperature on the NdOFeAs and the superconducting NdO_{1-x}F_xFeAs system ($T_c \sim 49$ K). Both samples are in their tetragonal phase and hence the differences reflect the effect of F-substitution. The L_3 -edge WL intensity shows a significant increase with F-doping, suggesting an increase of the localization of the RE empty d density of states [33]. In addition, a substantial change in peaks B_1 and B_2 can be seen (inset of figure 4).

Recently Sun *et al* [34] have studied CeO_{1-x}F_xFeAs by the Ce L_3 -XANES system as a function of external pressure, revealing a drastic decrease of the WL intensity while the T_c

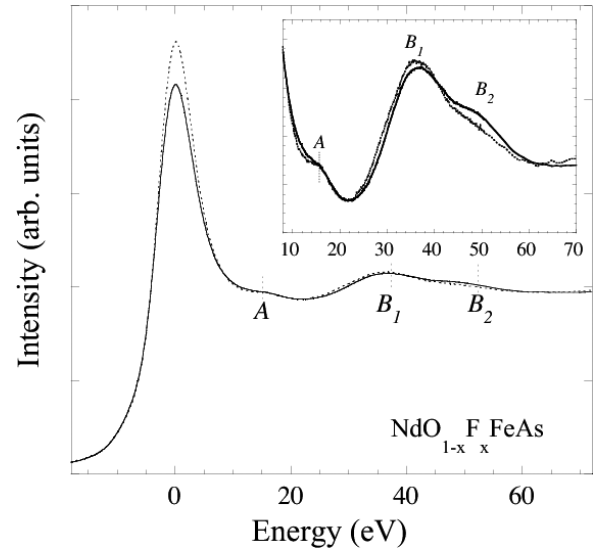


Figure 4. Nd L_3 -edge for the undoped (solid) and F-substituted (dotted) superconducting systems at room temperature. Both the samples are in their tetragonal phase and hence the differences are merely due to the F-insertion. The inset shows a zoom into the features A, peak B_1 and peak B_2 .

decreases with increasing hydrostatic pressure. Incidentally, the results reported here show a more intense Nd L_3 WL for the superconducting system, and hence the increased intensity (more atomic like character) of the L_3 WL may be somehow related to the superconductivity. It is possible that the F-substitution in the NdOFeAs causes reduced hybridization between the Nd 5d and admixed 4f orbitals, similar to the 4f-superconductors [35], in which the superconductivity gets suppressed with increased hybridization.

On the other hand, the peak B_1 seems to show a different effect of F-doping. Indeed, peaks B_1 and B_2 tend to merge (peak B_1 hardly shows any shift while peak B_2 appears at a lower energy) The doping of F induces an increase of Nd–O/F distance; hence the shift of the peak B_2 towards lower energy is reasonable. On the other hand, the diffraction data reveal a shrinkage of the RE–As bonds; hence a shift of the peak B_1 towards higher energy should be expected, inconsistent with the present results. This may be due to the fact that diffraction tends to average local distortions and is thus less sensitive to localized structural distortions and possible nanoscale inhomogeneities [36, 37].

In summary, we have studied the RE L_3 -XANES of the oxypnictides REOFeAs with variable rare earth ions to explore the valence electronic structure as well as the local geometry of the RE–O slab. While the L_3 white lines hardly show any change across the tetragonal to orthorhombic structural phase transition temperature, a clear change is observed in the spectral weight with the electron doping. In addition, the XANES features above the WL show a systematic change due to the varying local geometry with the rare earth size. The energy separation between the WL and the continuum resonances change consistently with a change of RE–As and RE–O distance, due to changing misfit between the FeAs and REO sub-layers. A systematic change of the relative intensities

of the continuum resonance features is also observed. Since the vertical position of the As atom changes systematically with the rare earth size (the As atom moves away from the Fe–Fe plane due to the decreased Fe–As–Fe angle with decreasing rare earth size [32]), this has a direct influence on the local geometry of the REO slabs, as demonstrated by the XANES spectra. The results suggest that the interlayer coupling between the Fe–As and the spacer (REO) layer may also play a role in the superconductivity mechanism of the REOFes. Thus, the outcome of this work recalls the recent debate on the misfit strain [5, 4] and out-of-plane disorder controlled superconductivity in copper oxide high T_c superconductors [22–24], bringing the two families onto the same platform for discussion. Although it is difficult to argue on the cause or consequence of the local structural changes and the quantitative role of intra and interlayer coupling in the correlating itinerant magnetism and superconductivity, the present results certainly add a new experimental feedback to understand the role of the structure and local chemistry in the fundamental properties of REOFes oxypnictides.

Acknowledgments

The authors thank the Elettra staff for their help and cooperation during the experimental run (proposal no. 20085317). We also acknowledge Zhong-Xian Zhao and Z A Ren (Beijing) for providing high quality samples for the present study. This research has been partially supported by the COMEPHS (FP6-STREP Controlling mesoscopic phase separation). One of us (BJ) would like to acknowledge the MIUR (Italy) for a fellowship under the Italy–India bilateral program.

References

- [1] Kamihara Y, Watanabe T, Hirano M and Hosono H 2008 *J. Am. Chem. Soc.* **130** 3296
- [2] Ricci A, Poccia N, Ciasca G, Fratini M and Bianconi A 2009 *J. Supercond. Nov. Magn.* **22** 589
- [3] Fratini M *et al* 2008 *Supercond. Sci. Technol.* **21** 092002
- [4] Bianconi A, Bianconi G, Caprara S, Di Castro D, Oyanagi H and Saini N L 2000 *J. Phys.: Condens. Matter* **12** 10655
Bianconi A, Agrestini S, Bianconi G, Di Castro D and Saini N L 2001 *J. Alloys Compounds* **317** 537
Agrestini S, Saini N L, Bianconi G and Bianconi A 2003 *J. Phys. A: Math. Gen.* **36** 9133
- [5] Poccia N and Fratini M 2009 *J. Supercond. Nov. Magn.* **22** 599
- [6] Agrestini S, Castro D D, Sansone M, Saini N L, Saccone A, Negri S D, Giovannini M, Colapietro M and Bianconi A 2001 *J. Phys.: Condens. Matter* **13** 11689
- [7] Ren Z A *et al* 2008 *Europhys. Lett.* **83** 17002
- [8] Ishida K, Nakai Y and Hosono H 2009 *J. Phys. Soc. Japan* **78** 062001
- [9] Zhao J *et al* 2008 *Nat. Mater.* **7** 953
- [10] Huang Q, Zhao J, Lynn J W, Chen G F, Luo J L, Wang N L and Dai P 2008 *Phys. Rev. B* **78** 054529
- [11] Zhao J *et al* 2008 *Phys. Rev. B* **78** 132504
- [12] De la Cruz C *et al* 2008 *Nature* **453** 899
- [13] Margadonna S, Takabayashi Y, McDonald M T, Brunelli M, Wu G, Liu R H, Chen X H and Prassides K 2009 *Phys. Rev. B* **79** 014503
Kasperkiewicz K, Bos J W G, Fitch A N, Prassides K and Margadonna S 2009 *Chem. Commun.* 707–9
- [14] See e.g., Proceedings of the International Symposium on Fe–Pnictide Superconductors 2008 *J. Phys. Soc. Japan* **77** (Suppl. C)
- [15] See e.g., focus issue on iron based superconductors 2009 *New J. Phys.* **11** 025003
- [16] See e.g., a short review by Izyumov Yu A and Kurmaev E Z 2008 *Phys.—Usp.* **51** 1261
- [17] Lee C-H, Iyo A, Eisaki H, Kito H, Fernandez-Diaz M T, Ito T, Kihou K, Matsuhata H, Braden M and Yamada K 2008 *J. Phys. Soc. Japan* **77** 083704
Miyazawa K, Kihou K, Shirage P M, Lee C-H, Kito H, Eisaki H and Iyo A 2009 *J. Phys. Soc. Japan* **78** 034712
Lee C-H *et al* 2008 *J. Phys. Soc. Japan* **77** 44
- [18] Bianconi A, Dell’Ariccia M, Durham P J and Pendry J B 1982 *Phys. Rev. B* **26** 6502
Bianconi A, Incoccia L and Stipcich S (ed) 1982 *EXAFS and Near Edge Structure* (Berlin: Springer)
Bianconi A 1988 *X-ray Absorption: Principles, Applications, Techniques of EXAFS, SEXAFS, XANES* ed R Prinze and D Koningsberger (New York: Wiley)
- [19] Journel L *et al* 2002 *Phys. Rev. B* **66** 045106 and references therein
- [20] Bianconi A, Marcelli A, Karnatak R, Dexpert H, Kotani A, Jo T and Petiau J 1987 *Phys. Rev. B* **35** 806
Chaboy J, Garcia J and Marcelli A 1997 *J. Magn. Magn. Mater.* **166** 149
- [21] Liu L, Gao B, Chu W, Chen D, Hu T, Wang C, Dunsch L, Marcelli A, Luo Y and Wu Z 2008 *Chem. Commun.* **4** 474–6
Fukui K, Ogasawara H, Kotani A, Harada I, Maruyama H, Kawamura N, Kobayashi K, Chaboy J and Marcelli A 2001 *Phys. Rev. B* **64** 104405
- [22] Eisaki H, Kaneko N, Feng D L, Damascelli A, Mang P K, Shen K M, Shen Z-X and Greven M 2004 *Phys. Rev. B* **69** 064512
Fujita K, Noda T, Kojima K M, Eisaki H and Uchida S 2005 *Phys. Rev. Lett.* **95** 097006
- [23] Sun C, Yang H, Cheng Lu, Wang J, Xu X, Ke S and Cao L 2008 *Phys. Rev. B* **78** 104518
- [24] Hobou H, Ishida S, Fujita K, Ishikado M, Kojima K M, Eisaki H and Uchida S 2009 *Phys. Rev. B* **79** 064507
- [25] Ren Z-A *et al* 2008 *Europhys. Lett.* **82** 57002
- [26] Di Gioacchino D, Marcelli A, Zhang S, Fratini M, Poccia N, Ricci A and Bianconi A 2009 *J. Supercond. Nov. Mag.* **22** 549–52
- [27] Bianconi A, Dell’Ariccia M, Gargano A and Natoli C R 1983 *EXAFS and Near Edge Structure* ed A Bianconi, L Incoccia and S Stipcich (Berlin: Springer) p 57
Bianconi A, Fritsch E, Calas G and Petiau J 1985 *Phys. Rev. B* **32** 4292
- [28] Ignatov A, Zhang C L, Vannucci M, Croft M, Tyson T A, Kwok D, Qin Z and Cheong S-W 2008 arXiv:0808.2134
- [29] Tan Z, Filipkowski M E, Budnick J I, Heller E K, Brew D L, Chamberland B L, Bouldin C E, Woicik J C and Shi D 1990 *Phys. Rev. Lett.* **64** 2715
Tan Z, Budnick J I, Chen W Q, Brew D L, Cheong S-W, Cooper A S and Rupp L W 1990 *Phys. Rev. B* **42** 4808
Tan Z, Budnick J I, Luo S, Chen W Q, Cheong S-W, Cooper A S, Canfield P C and Fisk Z 1991 *Phys. Rev. B* **44** 7008
Tan Z, Heald S M, Cheong S-W, Cooper A S and Budnick J I 1992 *Phys. Rev. B* **45** 2593
- [30] Wu Z Y, Benfatto M and Natoli C R 1992 *Phys. Rev. B* **45** 531
Wu Z Y, Benfatto M and Natoli C R 1998 *Phys. Rev. B* **57** 10336
- [31] Mustre de Leon J, Lezama-Pacheco J, Bianconi A and Saini N L 2009 *J. Supercond. Nov. Mag.* **22** 579–83
- [32] Iadecola A, Agrestini S, Filippi M, Simonelli L, Fratini M, Joseph B, Mahajan D and Saini N L 2009 *Europhys. Lett.* **87** 26005
- [33] Chaboy J, Marcelli A, Marziali M, Gzowski O, Stizza S and Szaniawska K 1993 *Japan. J. Appl. Phys.* **32** (Suppl. 32-2) 797
- [34] Sun L *et al* 2009 arXiv:0907.4212v1

-
- [35] Onuki Y and Kitaoka Y (ed) 2007 *J. Phys. Soc. Japan* **76** 051001 special issue of Frontiers of Novel Superconductivity in Heavy Fermion Compounds see also, a brief review by Steglich F 2005 *J. Phys. Soc. Japan* **74** 167
- [36] Zhang C J, Oyanagi H, Sun Z H, Kamihara Y and Hosono H 2008 *Phys. Rev. B* **78** 214513
- [37] Sato M, Kobayashi Y, Lee S-C, Takahashi H and Miura Y 2009 arXiv:0907.3007v1